Mechanical properties and melting conditions of beeswax for comb foundation forming

Tipapon Khamdaeng [1*], Thanasit Wongsiriamnuay [1], Numpon Panyoyai [1], Kanjana Narkprasom [1], and Weeranut Intagun [2]

(1 Faculty of Engineering and Agro-Industry, Maejo University, Chiang Mai, Thailand
2 Faculty of Engineering and Industrial Technology, Silpakorn University, Nakhon Pathom, Thailand)

Abstract: The melting conditions and the mechanical properties of beeswax after melting process were investigated in this study. The study variables of melting process were hot water temperature, propeller speed and time. The empirical model of beeswax melting efficiency was then established. The melting conditions were optimized based on the melting efficiency and color of beeswax and were found at the hot water temperature in range of 98 ℃ -100 ℃, propeller speed in range of 40-90 r/min and time in range of 12-15 min. The beeswax was solidified at the different cooling rates. The compression tests were performed at condition of 60% strain to characterize the mechanical behavior of beeswax. The constitutive equation for hyperelastic material was employed for beeswax. The two forms of the constitutive equation showed a better fit to the experimental data and the optimized material parameters were obtained. The rolling beeswax sheets were simulated under the different conditions of pressure angle, velocity and friction coefficient in order to determine the effect of the variables on the mechanical properties of beeswax sheet. The stress and deformation distributions across the beeswax sheet including the forces acting on the contact interfaces were examined. The pressure angle was found to be the most effective variable on the stress distribution. The maximum pressure angle of 11 °was found to provide the non-defect beeswax sheet. This present model for beeswax sheet rolling provides the understanding of the stress and deformation distributions and has been utilized to design the rolling for comb foundation forming.

Keywords: beeswax manufacture, comb foundation, material parameter, mechanical testing

Citation: Khamdaeng, T., T. Wongsiriamnuay, N. Panyoyai, K. Narkprasom, and W. Intagun. 2016. Mechanical properties and melting conditions of beeswax for comb foundation forming. Agricultural Engineering International: CIGR Journal, 18(3):282-293.

1 Introduction

Beeswax is the one of the animal waxes which be utilized in various industrial applications such as pharmaceutics, cosmetics, candle, comb foundation, and food industry (Altamirano-Fortoul et al., 2015; Attama et al., 2006; Bogdanov, 2009b; Gerginova et al., 2013; Medici et al., 2012; Monedero et al., 2009; Polat et al., 2013). Pure beeswax color is white or yellow to yellow brown, depending on relative quantity of pollen and propolis pigments. The wax extraction can be divided into melting and chemical extraction methods (Bogdanov, 2004; Sin et al., 2014). The prior one is less contaminate and not reacts with chemical compositions. The beeswax is melted using the thermal energy from hot water, steam, solar or electrical powers. The general melting extractors are hot water and steam. The electrical and solar heat supplied methods are used since they are not complicate to design and manufacture the melter system. Regarding different densities, the beeswax is separated by boiling in water or steam, and then filtering or pressing. Stainless steel or aluminium containers are suitable and the beeswax should not directly contact the heat source to avoid the darkening (Bogdanov, 2009a). In order to improve the beeswax production, the thermal distribution should be uniformed, not use too high temperature and not take too long time for melting. The simple way is setup of the propeller in the system. The effect of

Received date: 2016-03-12 Accepted date: 2016-08-02
***Corresponding author: Tipapon Khamdaeng,** Faculty of Engineering and Agro-Industry, Maejo University, Chiang Mai, Thailand. Email: tipapon@mju.ac.th

propeller speed has not been reported on the thermal distribution or melting duration of beeswax during melting process.

Beeswax structure is crystalline at lower temperature. Increasing temperature causes structural changes of beeswax (Espolov et al., 2014). Beeswax absorbs the thermal as applied energy. Since energy starts affecting the intermolecular bonds, the melting initially occurs. The studies of melting curves have been shown that the beeswax melting point producing from the different honeybee species is various (Buchwald et al., 2005). The melting point onset is in the wide range of 30 ℃ to 62 ℃ as same as the temperature range of the phase change is approximately between 18 ℃ to 32 ℃. The end of transition point in melting curve represents the melting of the major beeswax components. The different chemical constituents and contribution of the principal compound classes influence the amount energy required per unit mass for melting. The previous studies have been shown that the alteration of primary beeswax compounds such as fatty acids results in changes in the beeswax mechanical properties, i.e., compressive yield stress, stiffness and resilience (Buchwald et al., 2009). It is furthermore found that the differences of mechanical properties of beeswax correlate with the nesting ecology of the species (Buchwald et al., 2008). The moduli of elasticity of beeswax and synthetic waxes have been reported (Hossain et al., 2009). However, the waxes with less stiffness will exhibit more plasticity. The greater stiffness has been reported as a result of increasing strain rate (Buchwald et al., 2006). The applied load should be therefore taken into account for forming of comb foundation. The manufacturing of comb foundation is generally formed using either calendaring or casting methods (Bogdanov, 2009a). The prior one is preferred due to the smaller brittleness provided. In this study, as far as the melting process development is concerned, the variables, i.e., hot water temperature, time and propeller speed, are investigated. The mechanical properties of beeswax were determined for studying the effect of hot water temperature and cooling rate on the comb foundation calendaring. The various conditions are then further simulated to estimate the stress distribution of the beeswax sheet.

2 Materials and methods

The effect of aforementioned variables on beeswax melting process including physical and mechanical properties of beeswax after melting process was examined. Beeswax of Asian bees in the genus *Apis* was used in this study. The wax produced by the comb cappings was selected and collected in the summer from Saraphi district, Chiang Mai, Thailand. The experimental procedure, computational model, mathematical formulations and determination of material parameters of the beeswax sheet are described as follows.

2.1 Experimental procedure

Fifty grams of beeswax produced from comb cappings was used for each melting condition. The beeswax was melted in double boiler. Propeller was installed at the top of the boiler. Heat was generated from hot plate (IKA® model C-MAG HS 7, IKA-Works Asia, MY) and conducted to water which was used as a heat transfer medium. The hot water temperature was varied from 80 ℃ -100 ℃ and rotational speed of propeller used was in range of 0-150 r/min. Time varying between 5-15 min was considered. The contour plots of hot water temperature, time, and rotational speed of propeller versus melting efficiency were obtained to optimize the melting condition as well as the melting model. The melting efficiency, *EFF*, was defined as Equation 1:

$$\%EFF = \frac{M_i - M_f}{M_i} \times 100 \quad (1)$$

where M_i is initial mass of comb cappings (50 g) and M_f is mass of residual comb cappings after melting process.

The impure substances were removed afterwards by filtering. The pure beeswax was poured into a mold and then the two cooling mediums were used to cool down the beeswax with different cooling rates, i.e., air and water at room temperature (25 ℃).

As the pure beeswax solidified, it was removed from the mold. The beeswax color was investigated in L^*, a^*, b^* using spectrophotometer (Hunter Lab, Miniscan XE Plus 45/0 LAV, Reston, USA). The purity and hue angle, H^o, were calculated as follows by Equation 2 and Equation 3.

$$C^* = \sqrt{(a^*)^2 + (b^*)^2} \quad (2)$$

$$H^o = tan^{-1}(b^*/a^*) \quad (3)$$

where L^*, a^*, b^* and C^* indicates lightness, red/green coordinate, yellow/blue coordinate and chroma, respectively.

The beeswax was then punched into the circular cylinders with the diameter and height of 17 mm and 8 mm, respectively. The cylindrical specimens with optimized condition yielding melting efficiency more than 70% were allowed to test in compression at 25 ℃. The specimens were vertically placed on the platform of the mechanical testing (Texture analyzer model TA-XT2i Plus, Texture Technologies, Inc., UK) and subjected to compression by the flat surface probe with the diameter of 100 mm. The load with cross-head speed of 0.6 m/s was provided on the top surface of the cylindrical specimens. The compression test was performed until the strain reached 60% of initial specimen height. The stress and stretch relation was monitored and analyzed with nonlinear elastic model. The material parameters of beeswax were consequently estimated. These material parameters were used for the simulation of the beeswax sheet under various rolling conditions.

2.2 Computational model

The sheet geometry was set with a width of w = 200 mm, thickness s = 5 mm, and length L = 400 mm (Figure 1(a)). The roller diameter was 200 mm (Figure 1(b)). The schematic illustration of variables and forces acting on beeswax sheet surface during a rolling is shown in Figure 2. The pressure angles, θ, acting on the sheet surface were 9, 10 and 11 ° with forward velocities of v = 0.06, 0.08 and 0.1 m/s, respectively. The friction coefficients, μ, between the sheet and roller were furthermore assumed to be equal to 0.3, 0.6 and 0.9, respectively. The variables used as the rolling condition were summarized in Table 1. The sheet was assumed to be homogeneous, incompressible, and isotropic hyperelastic material undergoing the finite deformations and was modeled with density of ρ = 960 kg/m^3. The roller was assumed to be rolling on the flat sheet surface at any constant velocity with no slipping. The average stress and deformed thickness of beeswax sheet along the position lines L1-L11 (Figure 3) were estimated to display the average stress and strain distributions. The two-dimensional mechanical characterization of the beeswax sheet could describe the uniformity of the forces spreading across the beeswax sheet surface during a rolling.

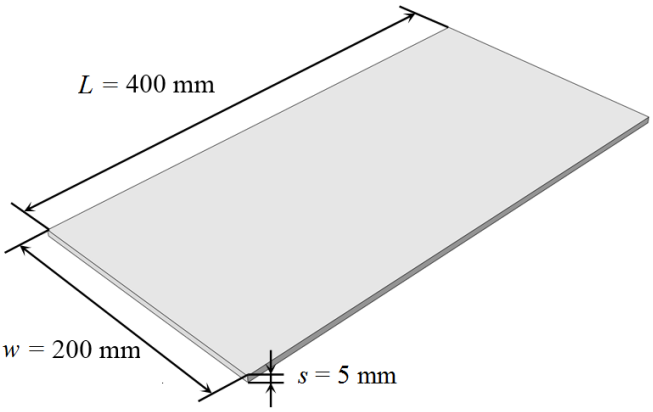

(a)

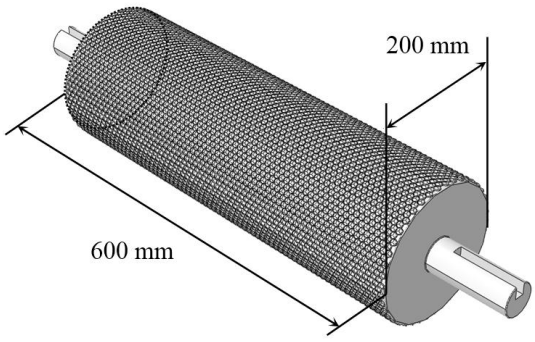

(b)

Figure 1 Schematic illustration of (a) beeswax sheet and (b) roller

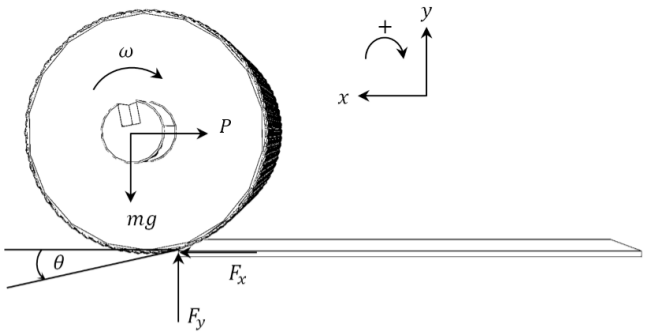

Figure 2 Schematic illustration of beeswax sheet during a rolling: Roller with pressure angle of θ rotates at ω in the direction shown. *P*, F_x, F_y and *mg* are the rolling force, resultant force in *x* direction, resultant force in *y* direction and gravitational force, respectively.

Table 1 The variables used as the rolling condition

Variables	Values
Pressure angle	9, 10 and 11 °
Rolling velocity	0.06, 0.08 and 0.1 m/s
Friction coefficient	0.3, 0.6 and 0.9

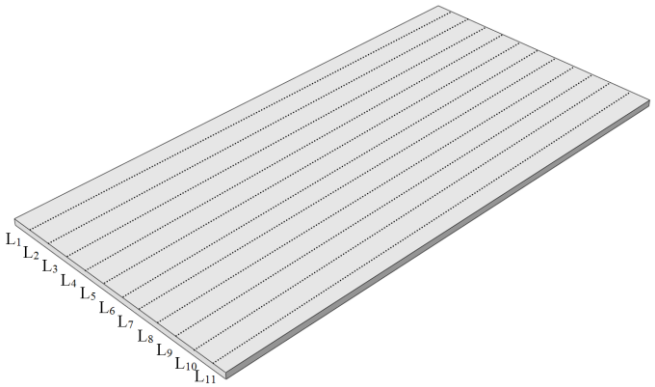

Figure 3 Schematic illustration of position lines L1-L11 on beeswax for measuring the average stress and strain distributions

2.3 Mathematical formulations

The law of conservation of mass following Equation 4 of continuity is

$$\frac{\partial \rho}{\partial t} + \frac{\partial \rho \boldsymbol{v}}{\partial \boldsymbol{x}} = 0 \qquad (4)$$

where ρ denotes a density of the beeswax which is a constant, $\boldsymbol{v}$ denotes the velocity vector and $\boldsymbol{x}$ denotes the position vector in deformed configuration.

The equation of motion representing the equilibrium at all points throughout the volume of the nonlinear elastic body with body forces is expressed by Equation 5

$$\frac{\partial \boldsymbol{\sigma}}{\partial \boldsymbol{x}} + \boldsymbol{X} = \rho \boldsymbol{a} \qquad (5)$$

where $\boldsymbol{\sigma}$ denotes the Cauchy stress tensor, $\boldsymbol{X}$ denotes the body forces within the beeswax and $\boldsymbol{a}$ denotes its acceleration. The Cauchy stress tensor can be written in term of the second Piola-Kirchhoff stress tensor, $\boldsymbol{S}$, as Equation 6:

$$\boldsymbol{\sigma} = J^{-1}\boldsymbol{F}\boldsymbol{S}\boldsymbol{F}^{T} \qquad (6)$$

where $\boldsymbol{F}$ denotes the deformation gradient tensor and J denotes the Jacobian determinant of the deformation gradient tensor.

Applying the chain rule, the second Piola-Kirchhoff stress tensor can be given in terms of the right Cauchy deformation tensor, $\boldsymbol{C}$, and the finite strain tensor, $\boldsymbol{E}$, as Equation 7:

$$\boldsymbol{S} = \frac{\partial \psi}{\partial \boldsymbol{C}} \frac{\partial \boldsymbol{C}}{\partial \boldsymbol{E}} \qquad (7)$$

where ψ denotes the strain energy function. The hyperelastic constitutive model, Yeoh strain energy function (Renaud et al., 2009), was used to describe the nonlinear response of beeswax. See Equation 8:

$$\psi = \sum_{i=1}^{3} c_i (I_1 - 3)^i \qquad (8)$$

where c is material (stress-like) parameter (details of material parameter estimation will describe in section 2.4) and I_1 denotes the first invariant of the right Cauchy deformation tensor, which is Equation 9:

$$I_1 = tr\boldsymbol{C} \tag{9}$$

The right Cauchy deformation tensor can be expressed in terms of the deformation gradient tensor with the indices $\boldsymbol{F}$ as Equation 10:

$$\boldsymbol{C} = \boldsymbol{F}^T\boldsymbol{F} \tag{10}$$

The deformation gradient tensor is the transformation of a material particle point, $\boldsymbol{X}(x, y, z)$, at the reference configuration, Ω_o, to a new position, $\boldsymbol{x}(x, y, z)$, which can be described by Equation 11:

$$\boldsymbol{F} = \frac{\partial \boldsymbol{x}}{\partial \boldsymbol{X}} \tag{11}$$

Furthermore, the von Mises stress, $\boldsymbol{\sigma_v}$, can be calculated from the Cauchy stress tensor, that is Equation 12:

$$\boldsymbol{\sigma_v} = \sqrt{3J_2} \tag{12}$$

where J_2 denotes the second deviatoric stress invariant, which is Equation 13:

$$J_2 = \frac{1}{2}\left[tr(\boldsymbol{\sigma}^2) - \frac{1}{3}tr(\boldsymbol{\sigma})^2\right] \tag{13}$$

2.4 Determination of material parameters

The material parameters were optimized by minimizing the difference between the theoretically and experimentally determined Cauchy stresses at each equilibrium configuration, k, defined as Equation 14:

$$\chi^2 = \sum_{k=1}^{n}(\sigma_k^{mod} - \sigma_k^{exp})^2 \tag{14}$$

where superscript mod and exp denote theoretical and experimental values, respectively. Since the theoretical values depend on the material parameters of the constitutive model, the material parameters were progressively estimated to minimize the objective function.

The minimization process was started by guessing material parameter values of constitutive functions and then iterating until the new values of the constitutive functions had not to be greater different from those of the previous iteration. A goodness of fit to data was used to calculate the correlation coefficient, R, between the theoretically and experimentally determined quantities, that is Equation 15:

$$R = \frac{\sum_{k=1}^{n}[(\sigma_k - \bar{\sigma})^{exp}(\sigma_k - \bar{\sigma})^{mod}]}{\sqrt{\sum_{k=1}^{n}[(\sigma_k - \bar{\sigma})^{exp}]^2}\sqrt{\sum_{k=1}^{n}[(\sigma_k - \bar{\sigma})^{mod}]^2}} \tag{15}$$

where the overbar denotes a mean value. R values should close to unity. The values, which were greater than 0.95 to 0.99, are suggested to be a good fit.

3 Results and discussion

3.1 Effect of hot water temperature, rotational speed of propeller and time on beeswax melting efficiency

This study aims at the investigation of the optimized conditions for melting and comb foundation forming of the beeswax. The contour plot was employed to monitor the effect of hot water temperature, rotational speed of propeller and time on the melting efficiency of beeswax (Figure 4). It was found that the melting efficiency of beeswax increases with the increasing temperature of hot water, rotational speed of propeller and time. Noted that, the melting efficiency of beeswax gradually increases until it reaches approximately 100 r/min beyond which

the efficiency is constant (Figures 4(a) and (c)). The uniformed thermal distribution was obtained in the melting process.

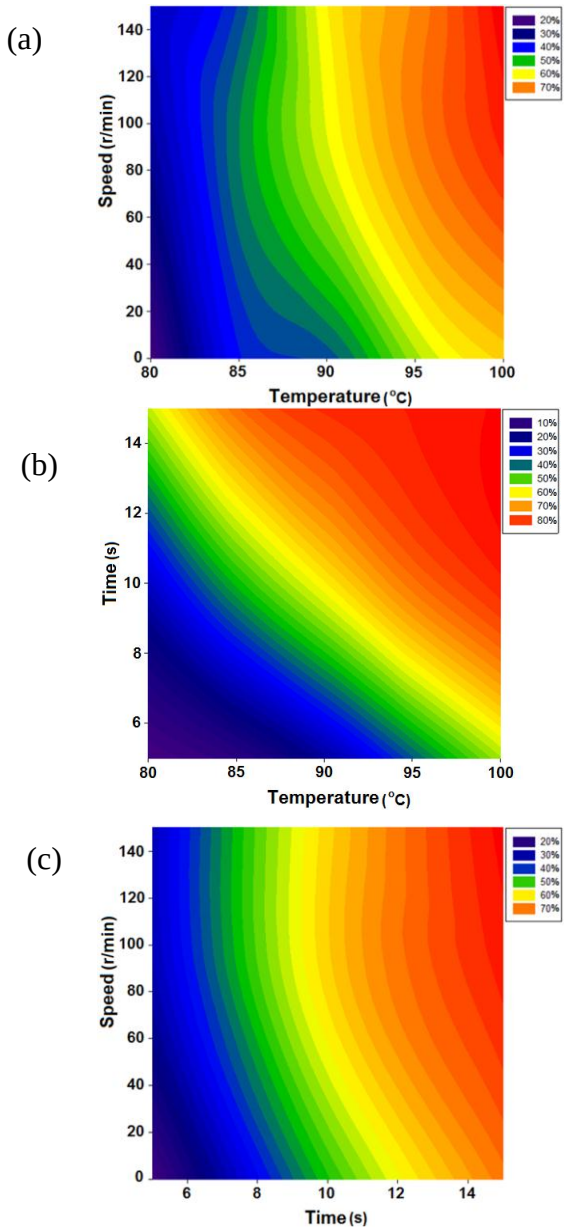

Figure 4 The beeswax melting efficiency at (a) rotational speed of propeller versus temperature, (b) time versus temperature and (c) rotational speed of propeller versus time

In this study, the relationship of melting efficiency of beeswax and three related variables (hot water temperature, rotational speed of propeller and time), as shown in Figures 4(a)-(c), can be fitted using a response surface analysis program. The linear relationship was found to be the best fitting function. The empirical model for beeswax melting efficiency was obtained as follows: $\%EFF_{mod} = 2.23T_w + 4.99t + 0.09\omega_p - 205.87$; where variables $\%EFF_{mod}$, T_w, t and ω_p are beeswax melting efficiency obtained from the model, hot water temperature, time and rotational speed of propeller, respectively. The comparison of the beeswax melting efficiency obtained from experiment ($\%EFF$) and empirical model ($\%EFF_{mod}$) at different temperatures, times and rotational speeds of propeller is respectively presented in Figures 5(a)-(c). The coefficient of variation was found to be equal to 0.216. The most accurate prediction was found at the hot water temperature of 100°C, time of 15 min and rotational speed of propeller of 100 r/min.

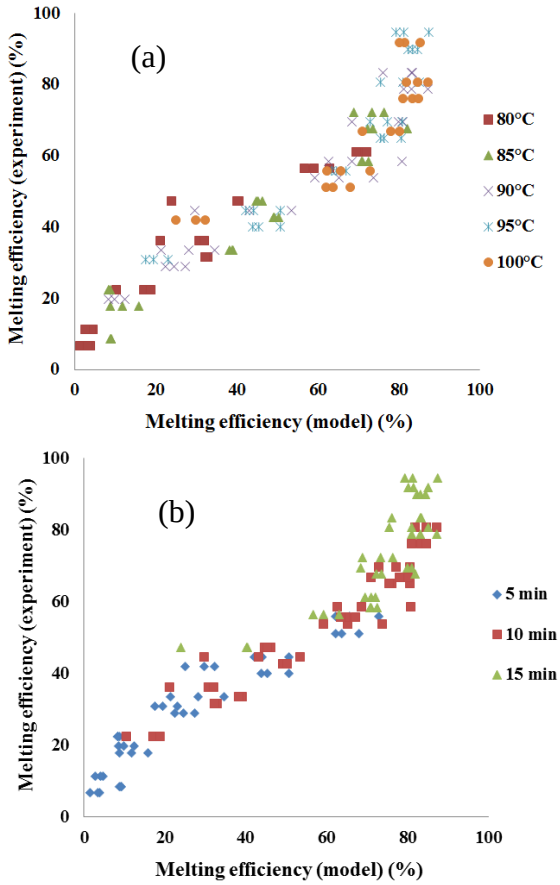

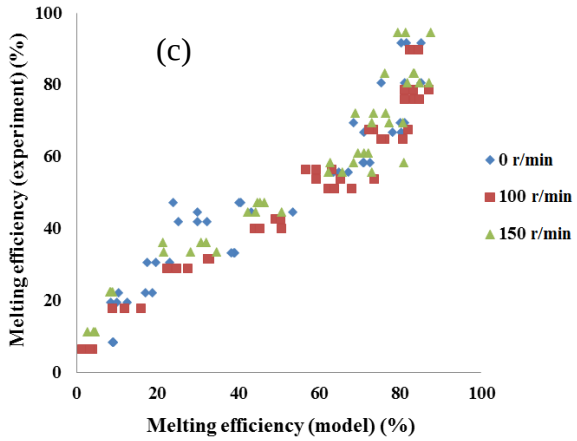

Figure 5 Comparison of the beeswax melting efficiency obtained from experiment and empirical model at different (a) temperatures, (b) times and (c) rotational speeds of propeller

The conditions yielding the melting efficiency more than 70% were hot water temperature in the range of 95 ^{o}C -100^{o}C, rotational speed of propeller in the range of 10-150 r/min and time in the range of 12-15 min. However, after the beeswax color and purity were investigated, we found that the hot water temperature range of 98 ^{o}C -100^{o}C, rotational speed of propeller range of 40-90 r/min and time range of 12-15 min were found as the condition providing the proper beeswax color (L^* $\geq$ 39, $C^* \geq 30.88$ and $45° \leq H^o \leq 90°$) and the high melting efficiency.

Beeswax is delicate for direct heat. Double boiler limits the maximum temperature of hot water, which the beeswax can reach, and maintains a steady heat transfer. Beeswax temperature was gradually changed resulted in unvarying beeswax color. Although, from the results, the hot water temperature and time did not affect the L^*, a^* and b^*, the L^* and b^* were found to decrease when the rotational speed of propeller increased. Therefore, the rotational speed of propeller was the most important variable in beeswax melting process, affecting thermal distribution and physical properties (color and purity) of beeswax.

3.2 Mechanical properties of beeswax

The Cauchy stress-strain relationships of beeswax were investigated after melting process at various melting and cooling conditions.

The maximum compressive stress and strain of beeswax cooling with different cooling rates are shown in Table 2. Air and water were used as cooling medium. The maximum compressive stress and strain of beeswax using cooling medium as water are not significantly higher than those using cooling medium as air ($p > 0.05$) as well as the hot water temperature was not found to affect the mechanical properties of beeswax after melting process (Table 3).

Table 2 The maximum compressive force and associated mechanical properties of beeswax cooling with different cooling mediums

Cooling medium at room temperature	Compressive force ,N	Compressive stress ,N/mm^2	Compressive strain ,%
Air	287.17 ± 18.70	1.27 ± 0.08	56.10 ± 2.22
Water	292.97 ± 15.24	1.29 ± 0.07	57.02 ± 2.27

Table 3 The maximum compressive force and associated mechanical properties of beeswax melting with different hot water temperatures

Hot water temperature , ℃	Compressive force ,N	Compressive stress ,N/mm^2	Compressive strain ,%
80	288.98 ± 14.33	1.27 ± 0.06	53.30 ± 2.86
85	298.29 ± 18.21	1.31 ± 0.08	55.90 ± 2.60
90	304.99 ± 16.49	1.34 ± 0.07	56.57 ± 2.47
95	309.57 ± 19.65	1.36 ± 0.09	55.86 ± 5.39
100	300.93 ± 31.71	1.33 ± 0.14	58.18 ± 1.35

The temperature of the cooling mediums was controlled at 25°C±2°C. Water has higher cooling rate than air because of its heat capacity. The mechanical properties, stress and strain, of beeswax were expected to be different between using air cooling and water cooling (Bourlieu et al., 2010; Jana and Martini, 2014). Although, the maximum compressive stresses and strains of beeswax were not significantly different (p > 0.05) between using air cooling and water cooling, the solidification time of beeswax using water cooling was smaller than that using air cooling, approximately 30 min of time difference. In the cooling process, water was suggested to use as the cooling medium since it has high cooling rate and it was easily obtainable and absolutely innocuous.

The Cauchy stress (true stress) is well-known stress measure and defined as the force acting on the material particle point of area in the deformed configuration (Basar and Weichert, 2000). The uniaxial Cauchy stress-stretch relationship of beeswax was quantitatively determined in this study. The similar trend as general nonlinear elastic material was obtained (Faghihi et al., 2014; Karimi et al., 2014; Khamdaeng et al., 2014). The stress-stretch behavior can be estimated using Equations 4-11. The Cauchy stress-stretch relationship of beeswax fitting with the hyperelastic constitutive model is shown in Figure 6. The relationship was established and separated into two relations. The c_1, c_2 and c_3 parameters for beeswax were determined following section 2.4. Three material parameters c_1 = 499.20, c_2 = -66.69 and c_3 = -273.47 for the elastic response and two material parameters c_1 = -471.06 and c_2 = -341.41 for the plastic response were obtained. The hyperelastic constitutive model with the optimized parameters fitted well both the elastic and plastic responses. The Pearson product moment correlation coefficient, R, was found to be equal to 0.985 and 0.962 for elastic and plastic responses, respectively.

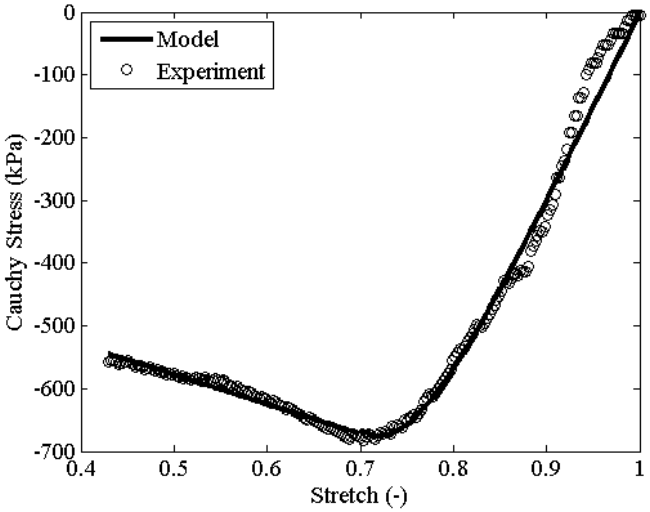

Figure 6 Cauchy stress and stretch relation of beeswax fitting with the hyperelastic constitutive model for elastic and plastic responses

3.3 Stress distribution of beeswax sheet

The rolling beeswax sheets were simulated under the different aforementioned conditions. The three material parameters of c_1 = 499.20, c_2 = -66.69 and c_3 = -273.47 for elastic response and two material parameters c_1 = -471.06 and c_2 = -341.41 for plastic response of beeswax were used. The von Mises stresses were calculated using Equation 12 and were plotted along the transversely locations of beeswax sheet as shown in Figure 7. The stress distribution dramatically increases with the increasing pressure angle and gradually increases with the increasing friction coefficient. The velocity was not found to affect the stress distribution.

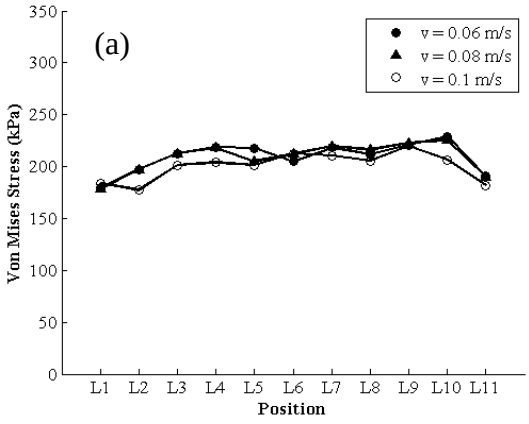

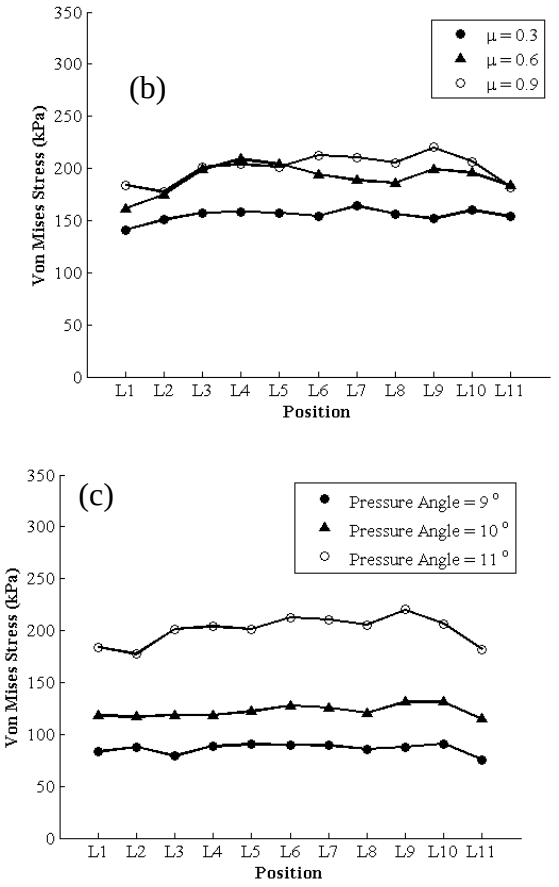

Figure 7 The von Mises stress distribution of beeswax with the rolling conditions of (a) pressure angle = 9 °and friction coefficient = 0.9, (b) pressure angle = 9 °and velocity = 0.1 m/s and (c) friction coefficient = 0.9 and velocity = 0.1 m/s at various positions

The displacement and associated deformed thickness distributions of beeswax, corresponding to the stress distributions at given conditions, are presented in Figure 8.

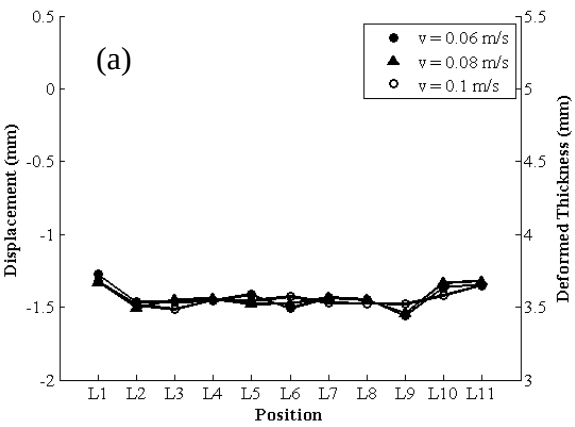

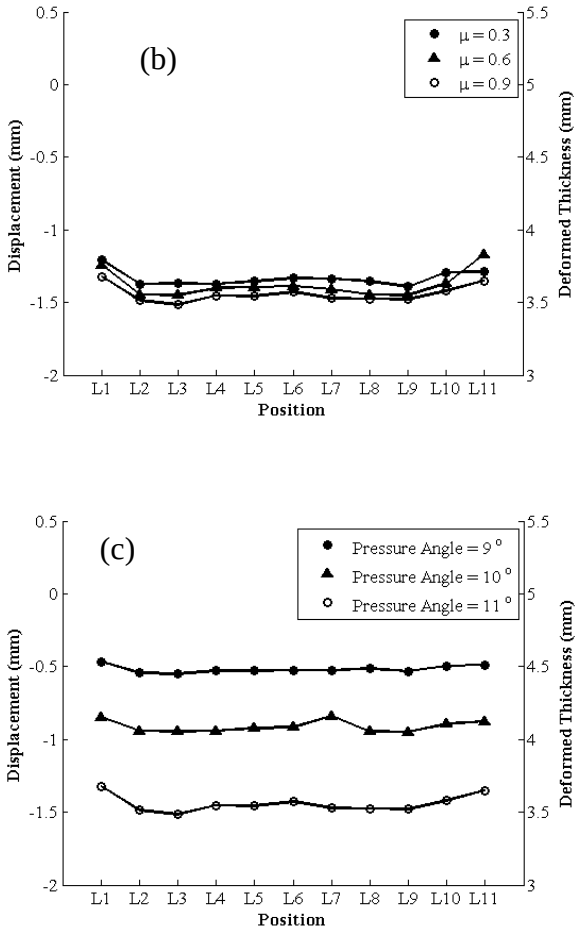

Figure 8 The displacement and associated deformed thickness distributions of beeswax with the rolling conditions of (a) pressure angle = 9 °and friction coefficient = 0.9, (b) pressure angle = 9 °and velocity = 0.1 m/s and (c) friction coefficient = 0.9 and velocity = 0.1 m/s at various positions

The beeswax sheet responded to stress by lengthening and thinning as shown in Figure 9 and Figure 10, respectively. The length and thickness of beeswax sheet (mean ± std) were respectively found to increase and decrease with the increasing pressure angle. The deformations of beeswax at different velocities and friction coefficients were not significantly different (p > 0.05).

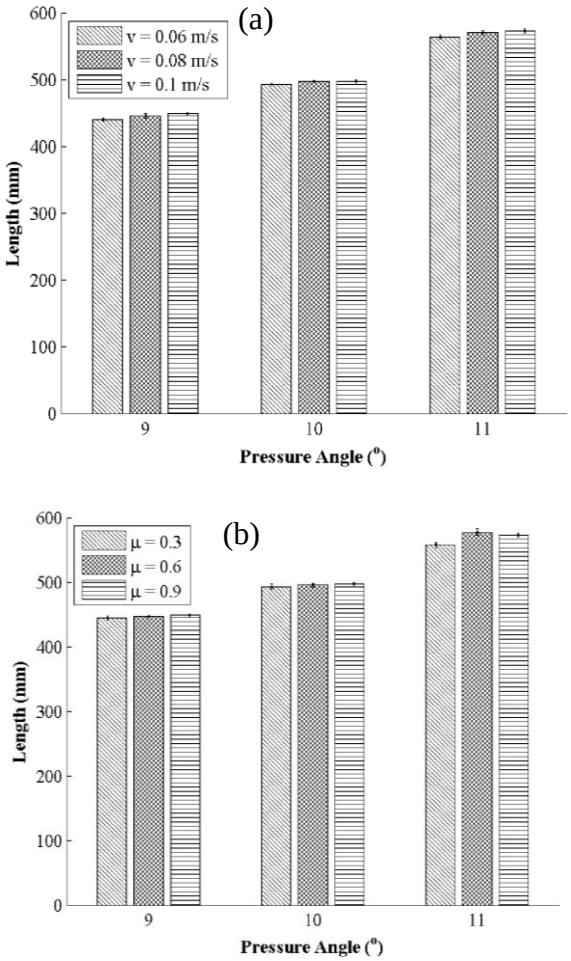

Figure 9 Comparison of the lengths of beeswax sheet of different (a) velocities and (b) friction coefficients at various pressure angles

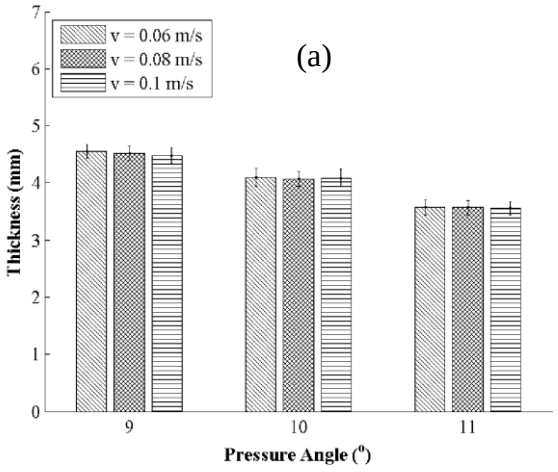

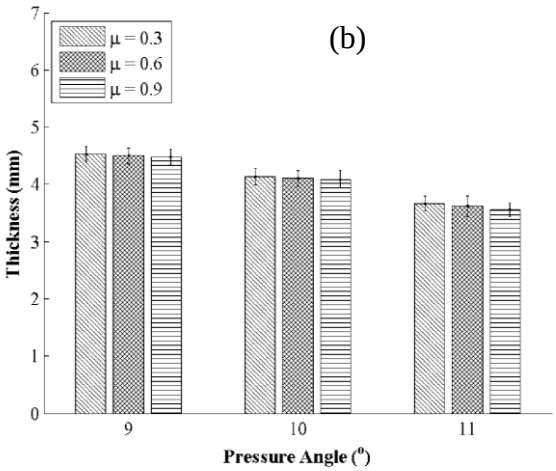

Figure 10 Comparison of the thicknesses of beeswax sheets of different (a) velocities and (b) friction coefficients at various pressure angles

In fact, the beeswax is subjected to a complex loading condition of rolling (Basti et al., 2014). The von Mises stress was applied in the present simulation. Given the Von Mises criterion, the stress distributions were estimated across the beeswax sheet surface in order to assure no failure occurred in the beeswax sheet structure (Figure 7). The non-uniform distribution increases with the increasing pressure angle. The pressure angle was not to exceed 11 ° because beyond which the maximum Von Mises stress was found to be higher than yield strength of beeswax. The beeswax sheet then has defects due to wavy edges and surface cracks. The displacement and associated deformed thickness of beeswax decrease with the increasing pressure angle (Figure 8). The minimum deformed thickness was approximately 3.5 mm (30% strain). The dimensions, length and thickness, of beeswax sheet after rolling were compared at various pressure angles with different rolling conditions. The similar trend of length versus pressure angle was found in every condition as shown in Figure 9, as same as the similar trend of thickness versus pressure angle was found in every condition (Figure 10). The width of beeswax sheet did not significantly change across the pressure angles and small edge variations were found for each condition. For this study, the pressure angle acting on the beeswax

surface plays a dominant role in the beeswax sheet forming or comb foundation forming. The rolling force had to be accounted for since forces at the contact interface mainly affected to the deformation (Bello, 2013; Samadi et al., 2014). The rolling force was found to increase with the increasing pressure angle and friction coefficient (Figure 11). Minus sign of the rolling force indicates the opposite of the given axis as shown in Figure 2. At high pressure angle of roller, in order to minimize the rolling force (or rolling resistance) in the beeswax sheet forming, the friction coefficient should be had a small value. Similarly, at high pressure of rolls in contact, the roller can be designed with the minimized diameter in order to decrease the contact surface between roller and beeswax sheet.

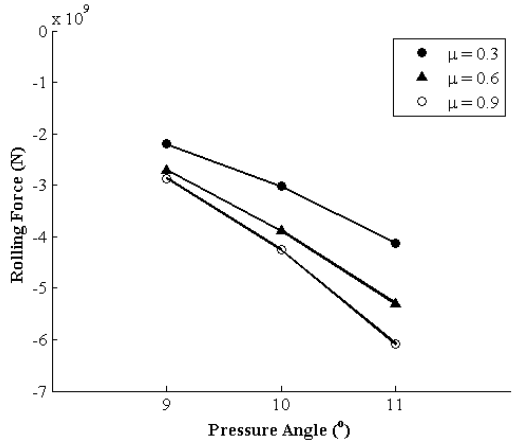

Figure 11 Rolling force versus pressure angle at different friction coefficients

The major advantages of this study are that the beeswax melting efficiency can be estimated using the present empirical model, incorporating the variables of the hot water temperature, rotational speed of propeller and time using the linear relation. The present optimized material parameters of beeswax can properly describe the mechanical behavior using the two suitable forms of the constitutive equation. In addition, the rolling force can be determined to serve as a design criterion. Although, the careful interpretation is required due to the certain limitations according to the model assumptions, the effect of variables on beeswax melting and forming are obtained for the process utilization.

4 Conclusion

The effect of the hot water temperature, rotational speed of propeller and time on beeswax melting was investigated. The linear relation of the beeswax melting efficiency and three related variables was established. The beeswax melting conditions were determined based on the obtained melting efficiency and color of beeswax. The cooling rate of beeswax after melting was considered in this study. The stress-stretch relationship of beeswax was investigated. The beeswax was treated as hyperelastic material and was modeled using the two forms of the constitutive equation. The optimized material parameters of beeswax were obtained. The simulation of beeswax sheet rolling was performed to determine the effect of the velocity, pressure angle and friction coefficient on the mechanical properties of beeswax sheet. The rotational speed of propeller and the pressure angle of roller were respectively found to be the relevant variables for beeswax melting and forming processes.

Acknowledgments

This study was supported by the Faculty of Engineering and Agro-Industry, Maejo University, Chiang Mai, Thailand. The authors are also grateful to Waranya Fuengchoom, Saifon Setila and Artit Dujeto for all additional helpful data.

References

Altamirano-Fortoul, R., P. Hernández-Muñoz, I. Hernando, and C. M. Rosell. 2015. Mechanical, microstructure and permeability properties of a model bread crust: Effect of different food additives. *Journal of Food Engineering*, 163: 25-31.

Attama, A. A., B. C. Schicke, and C. C. Müller-Goymann. 2006. Further characterization of theobroma oil–beeswax admixtures as lipid matrices for improved drug delivery systems. *European Journal of Pharmaceutics and Biopharmaceutics*, 64(3): 294-306.

Basar, Y., and D. Weichert. 2000. *Nonlinear Continuum Mechanics of Solids*. Berlin, Springer-Verlag.

Basti, A., S. Sojodi, S. Esmaeili, and M. Alitavoli. 2014. Development a predictive finite element model for

investigation of phases behavior after cold rolling process. *International Journal of Engineering*, 27(3): 425-430.

Bello, S. R. 2013. Development and evaluation of metal rolling machine for small-scale manufacturers. *Agricultural Engineering International: CIGR Journal*, 15(3): 80-85.

Bogdanov, S. 2004. Quality and standards of pollen and beeswax. *Apiacta*, 38: 334-341.

Bogdanov, S. 2009. Beeswax: Production, properties, composition and control. *Bee Product Science. The Beeswax Book*: 1-17.

Bogdanov, S. 2009. Beeswax: Uses and trade. *Bee Product Science. The Beeswax Book*: 1-16.

Bourlieu, C., V. Guillard, M. Ferreira, H. Powell, B. Valles-Pamies, S. Guilbert, and N. Gontard. 2010. Effect of cooling rate on the structural and moisture barrier properties of high and low melting point fats. *Journal of American Oil Chemists' Society*, 87(2): 133-145.

Buchwald, R., M. D. Breed, L. Bjostad, B. E. Hibbard, and A. R. Greenberg. 2009. The role of fatty acids in the mechanical properties of beeswax. *Apidologie*, 40(5): 585-594.

Buchwald, R., M. D. Breed, and A. R. Greenberg. 2008. The thermal properties of beeswaxs: unexpected findings. *The Journal of Experimental Biology*, 211(Pt 1): 121-127.

Buchwald, R., M. D. Breed, A. R. Greenberg, and G. Otis. 2006. Interspecific variation in beeswax as a biological construction material. *The Journal of Experimental Biology*, 209(20): 3984-3989.

Buchwald, R., A. R. Greenberg, and M. D. Breed. 2005. A Biomechanical perspective on beeswax. *American Entomologist*, 51(1): 39-41.

Espolov, T., J. Ukibayev, D. Myrzakozha, P. Perez-Lopez, and Y. Ermolaev. 2014. Physical and chemical properties and crystal structure transformation of beeswax during heat treatment. *Natural Science*, 6(11): 871-877.

Faghihi, S., A. Karimi, M. Jamadi, R. Imani, and R. Salarian. 2014. Graphene oxide/poly(acrylic acid)/gelatin nanocomposite hydrogel: Experimental and numerical validation of hyperelastic model. *Materials Science and Engineering: C*, 38: 299-305.

Gerginova, N., E. Ivanova, K. Bozhanchev, S. Geneva, and A. Tachev. 2013. Survey and health assessment of new cosmetic product based on natural ingredients. *Bulgarian Journal of Agricultural Science*, 19(2): 204-207.

Hossain, M. E., C. Ketata, and M. R. Islam. 2009. A comparative study of physical and mechanical properties of natural and synthetic waxes for developing models for drilling applications. *Journal of Characterization and Development of Novel Materials*, 1(3): 189-206.

Jana, S., and S. Martini. 2014. Effect of high-intensity ultrasound and cooling rate on the crystallization behavior of beeswax in edible oils. *Journal of Agricultural and Food Chemistry*, 62(41): 10192-10202.

Karimi, A., M. Navidbakhsh, and M. Haghpanahi. 2014. Constitutive model for numerical analysis of polyvinyl alcohol sponge under different strain rates. *Journal of Thermoplastic Composite Materials*, 1-10.

Khamdaeng, T., N. Panyoyai, and T. Wongsiriamnuay. 2014. Material parameter of rubber glove vulcanized using combined infrared and hot-air heating. *American Journal of Applied Sciences*, 11(4): 648-655.

Medici, S. K., A. Castro, E. G. Sarlo, J. M. Marioli, and M. J. Eguaras. 2012. The concentration effect of selected acaricides present in beeswax foundation on the survival of Apis mellifera colonies. *Journal of Apicultural Research*, 51(2): 164-168.

Monedero, F. M., M. J. Fabra, P. Talens, and A. Chiralt. 2009. Effect of oleic acid–beeswax mixtures on mechanical, optical and water barrier properties of soy protein isolate based films. *Journal of Food Engineering*, 91(4): 509-515.

Polat, S., M.-K. Uslu, A. Aygün, and M. Certel. 2013. The effects of the addition of corn husk fibre, kaolin and beeswax on cross-linked corn starch foam. *Journal of Food Engineering*, 116(2): 267-276.

Renaud, C., J.-M. Cros, Z.-Q. Feng, and B. Yang. 2009. The Yeoh model applied to the modeling of large deformation contact/impact problems. *International Journal of Impact Engineering*, 36(5): 659-666.

Samadi, A., M. Razzaghi Kashani, and M. H. N. Famili. 2014. Design, construction, and evaluation of a modified rolling pendulum to measure energy dissipation in rubber. *Polymer Testing*, 35(5): 56-61.

Sin, E. H. K., R. Marriott, A. J. Hunt, and J. H. Clark. 2014. Identification, quantification and Chrastil modelling of wheat straw wax extraction using supercritical carbon dioxide. *Comptes Rendus Chimie*, 17(3): 293-300.